

Electronic Supplementary Information

A Ru(II)-Arene-Ferrocene Complex With Promising Antibacterial Activity

Stephen Mensah,<sup>a</sup> Joseph D. Rosenthal,<sup>a</sup> Mamta Dagar,<sup>c</sup> Tyson Brown,<sup>a</sup> Jonathan J. Mills,<sup>a</sup> Christopher G. Hamaker,<sup>a</sup> Gregory M. Ferrence,<sup>a</sup> Michael I. Webb<sup>a,b\*</sup>

<sup>a</sup> Department of Chemistry, Illinois State University, Normal, IL, 61790

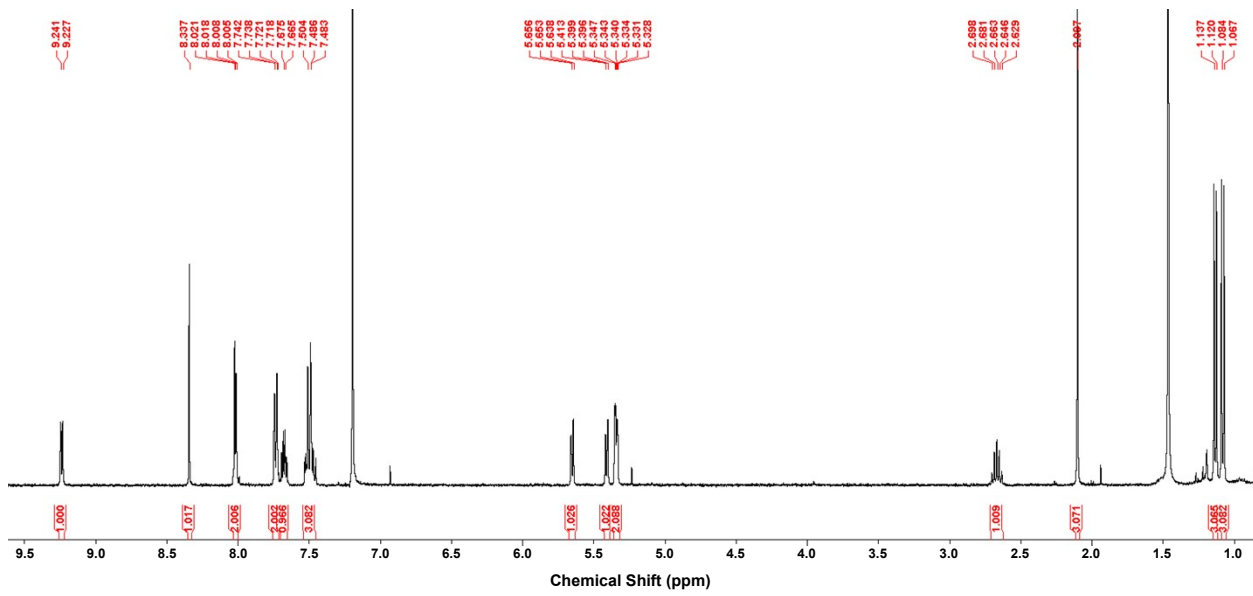
<sup>b</sup> Department of Chemistry, SUNY Geneseo, Geneseo, NY, 14454

<sup>c</sup> Department of Chemistry, University of Rochester, Rochester, NY, 14627

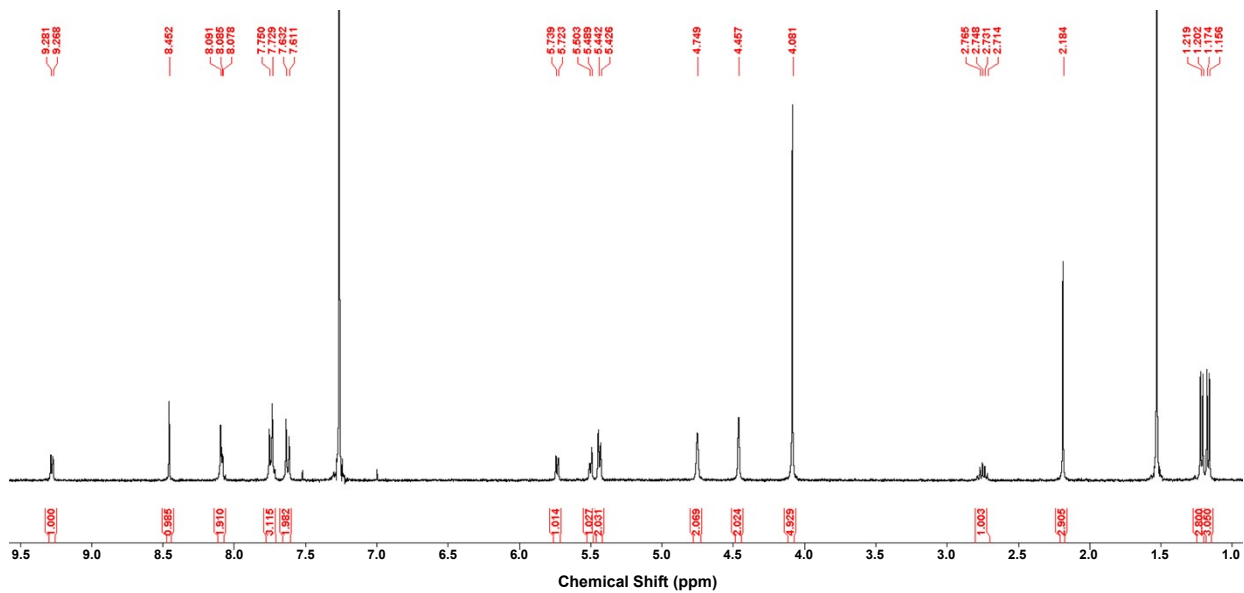
Corresponding Author: Michael I. Webb, [mwebb@geneseo.edu](mailto:mwebb@geneseo.edu)

Table of Contents:

- **Figures S1-S3:**  $^1\text{H}$  NMR spectra for the prepared Ru(II) complexes.
- **Figures S4-S6:**  $^{13}\text{C}$  NMR spectra for the prepared Ru(II) complexes.
- **Figures S7-S9:** Cyclic voltammograms for the prepared Ru(II) complexes.
- **Figures S10-S12:** UV-Vis spectra for the prepared Ru(II) complexes.
- **Figures S13-S16:**  $^1\text{H}$  NMR spectra for the prepared complexes in  $\text{D}_2\text{O}$  and  $\text{D}_6\text{-DMSO}$  following prolonged incubation at 37°C.
- **Figures S17-S19:** Fluorescence emission spectra at various complex-to-HSA ratios.
- **Figures S20-S22:** UV-Vis spectra for the prepared Ru(II) complexes with HSA.
- **Figures S23-S25:** UV-Vis spectra for the prepared Ru(II) complexes with CT-DNA.
- **Figures S26-S29:** UV-Vis spectra for the titration of the prepared Ru(II) complexes with CT-DNA and plots of  $[\text{DNA}] / (\varepsilon_A - \varepsilon_F)$  versus  $[\text{DNA}]$ .
- **Figures S30-S32:** Calibration curves for each complex to determine the extinction coefficients for each free complex.
- **Table S1.** Crystallographic data for complexes **C1** and **C3**.



**Figure S1.**  $^1\text{H}$  NMR of **C1** in  $\text{CDCl}_3$ .



**Figure S2.**  $^1\text{H}$  NMR of **C2** in  $\text{CDCl}_3$ .

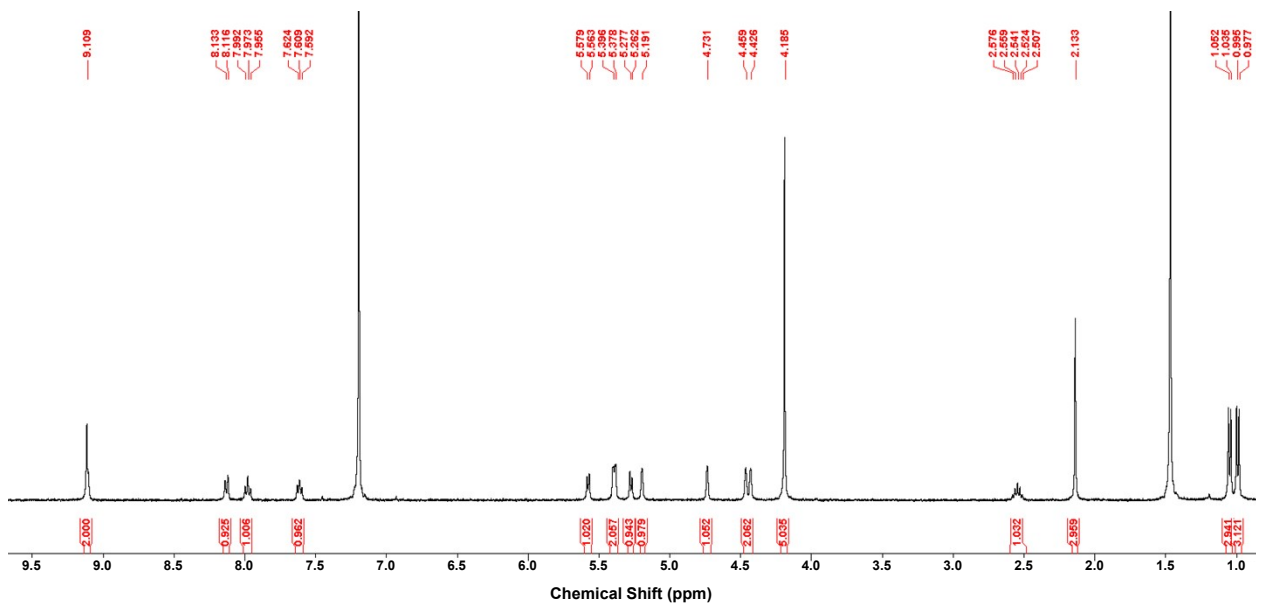


**Figure S3.**  $^1\text{H}$  NMR of **C3** in  $\text{CDCl}_3$ .

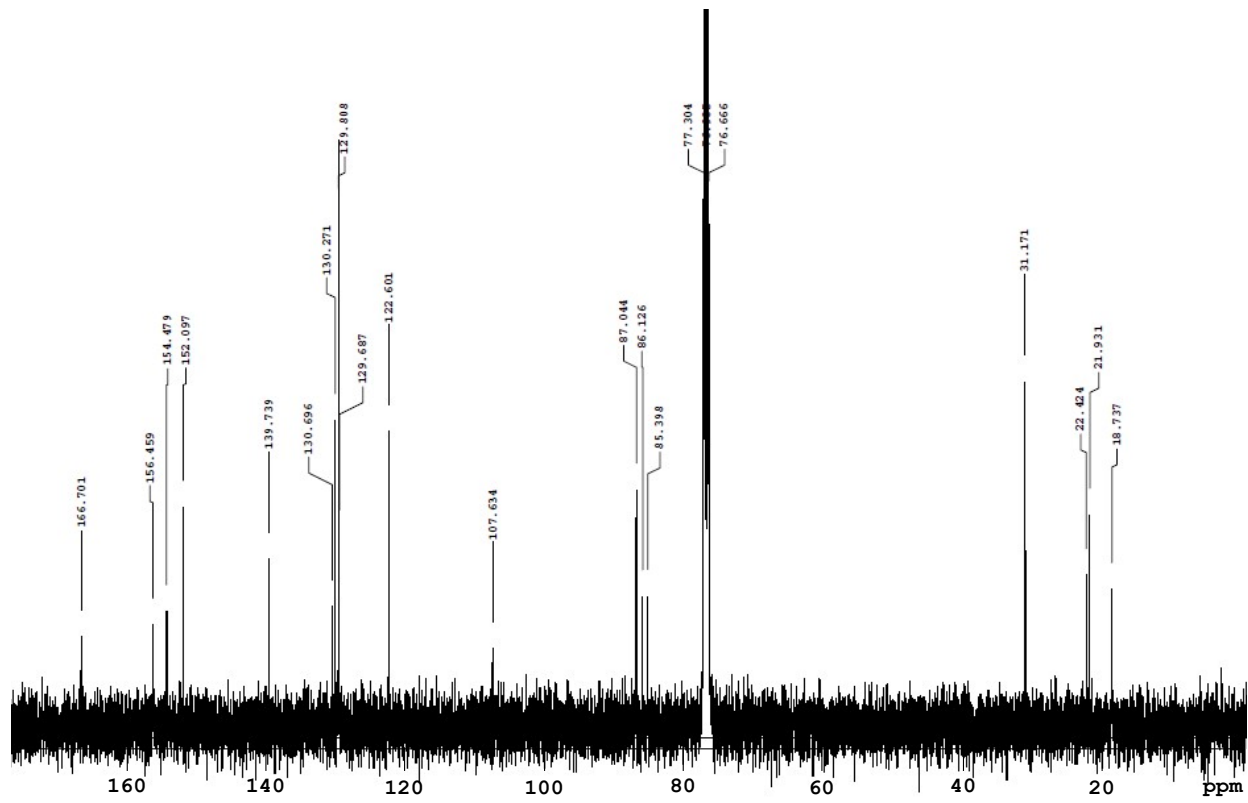


**Figure S4.**  $^{13}\text{C}$  NMR of C1 in  $\text{CDCl}_3$ .

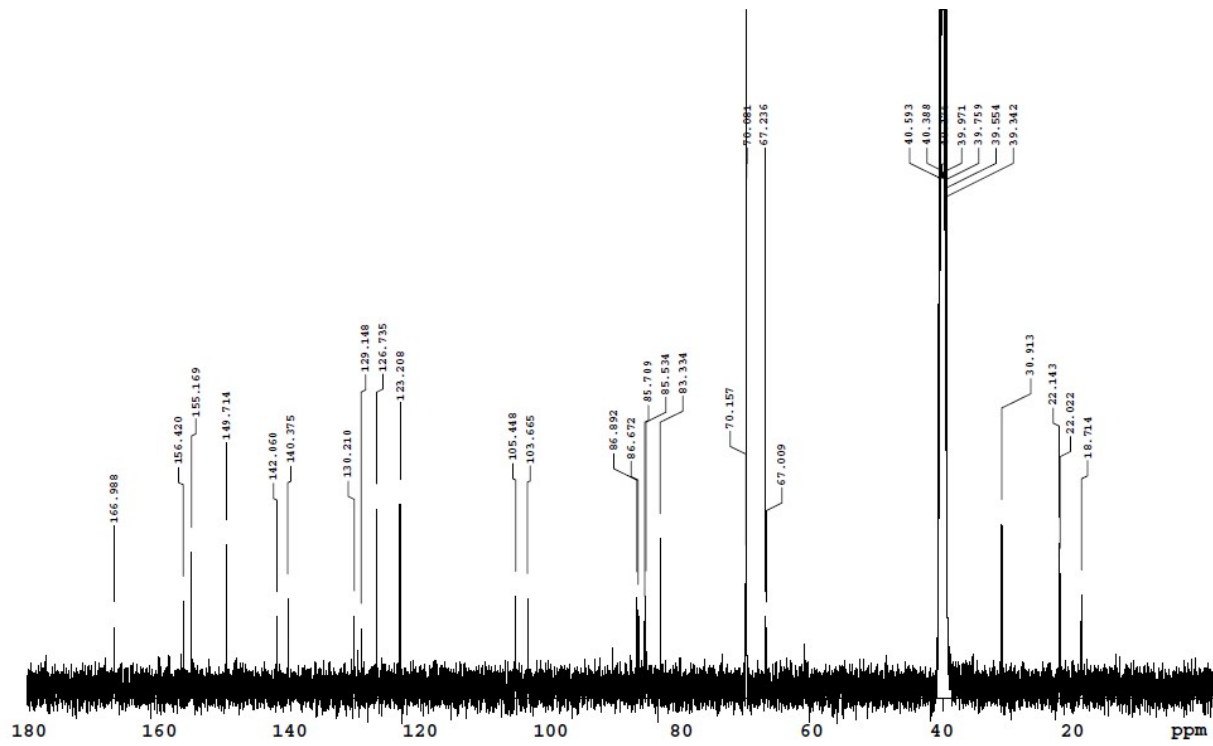


**Figure S5.**  $^{13}\text{C}$  NMR of C2 in  $\text{D}_6\text{-DMSO}$ .

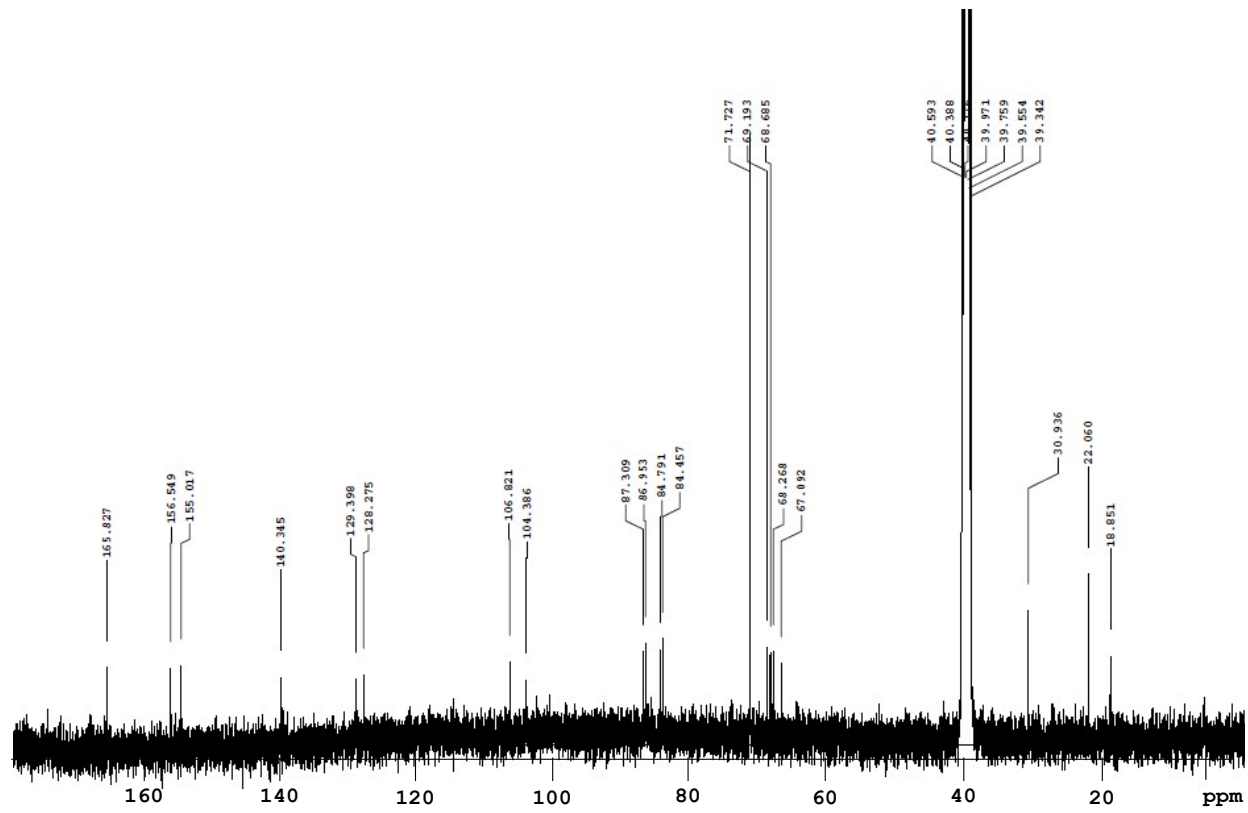


**Figure S6.**  $^{13}\text{C}$  NMR of C3 in  $\text{D}_6\text{-DMSO}$ .

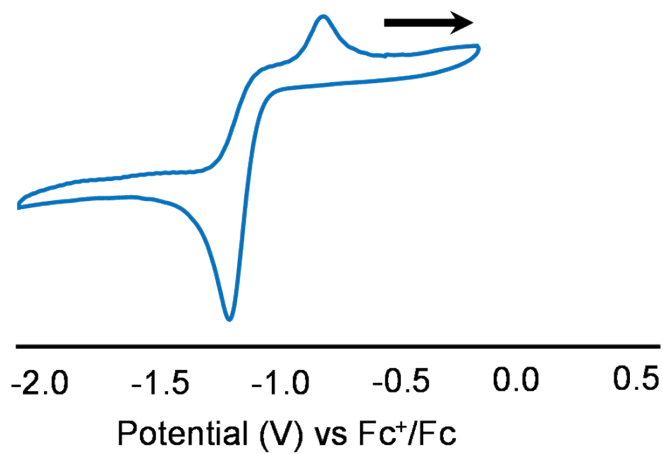


**Figure S7.** Cyclic voltammogram of **C1** (1 mM) in CH<sub>2</sub>Cl<sub>2</sub> containing 0.1 M [NBu<sub>4</sub>][PF<sub>6</sub>], where the scan direction is indicated by the arrow. An irreversible redox couple was observed with reduction potentials of -0.80 V and -1.23 V.

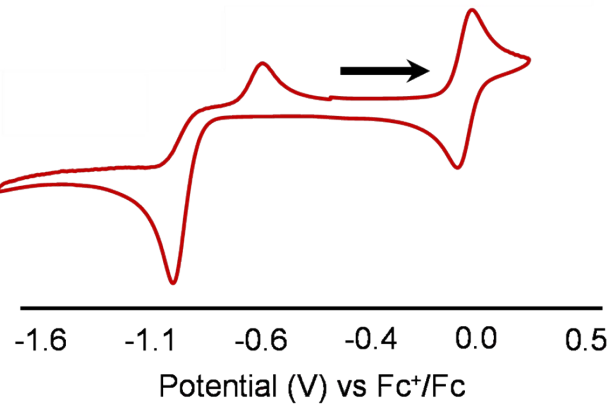


**Figure S8.** Cyclic voltammogram of **C2** (1 mM) in CH<sub>2</sub>Cl<sub>2</sub> containing 0.1 M [NBu<sub>4</sub>][PF<sub>6</sub>], where the scan direction is indicated by the arrow.

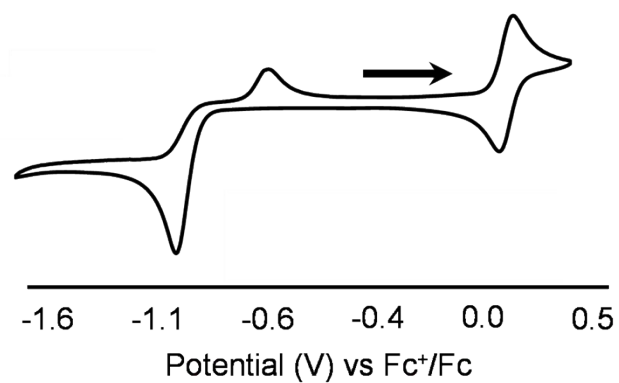


**Figure S9.** Cyclic voltammogram of **C3** (1 mM) in CH<sub>2</sub>Cl<sub>2</sub> containing 0.1 M [NBu<sub>4</sub>][PF<sub>6</sub>], where the scan direction is indicated by the arrow.

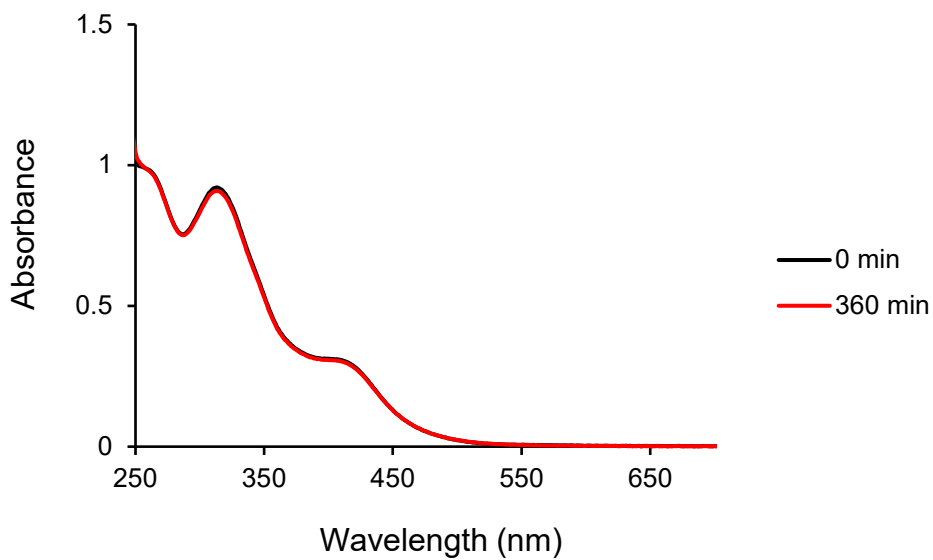


**Figure S10.** UV-Vis spectra of complex **C1** (100  $\mu$ M) incubated in PBS (pH 7.4) at 37 °C for 6 hours.

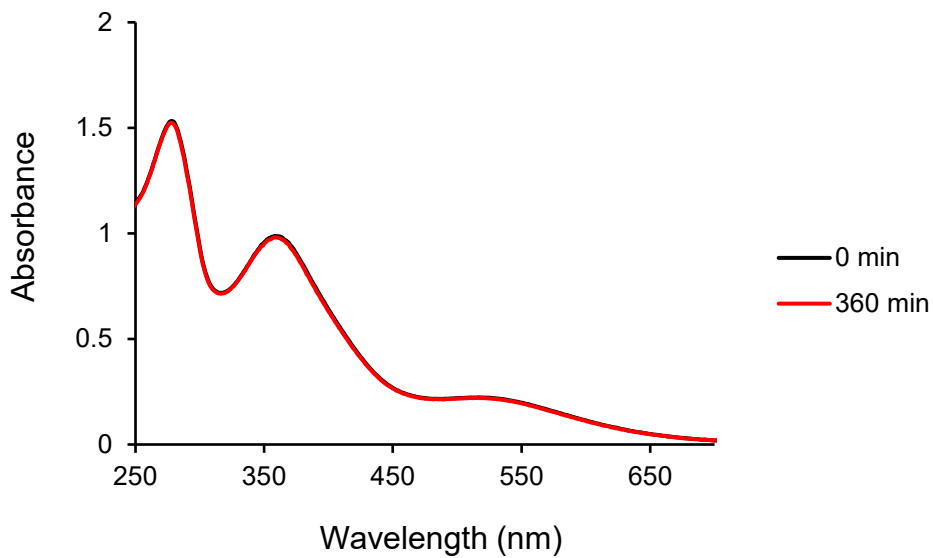


**Figure S11.** UV-Vis spectra of complex **C2** (100  $\mu$ M) incubated in PBS (pH 7.4) at 37 °C for 6 hours.

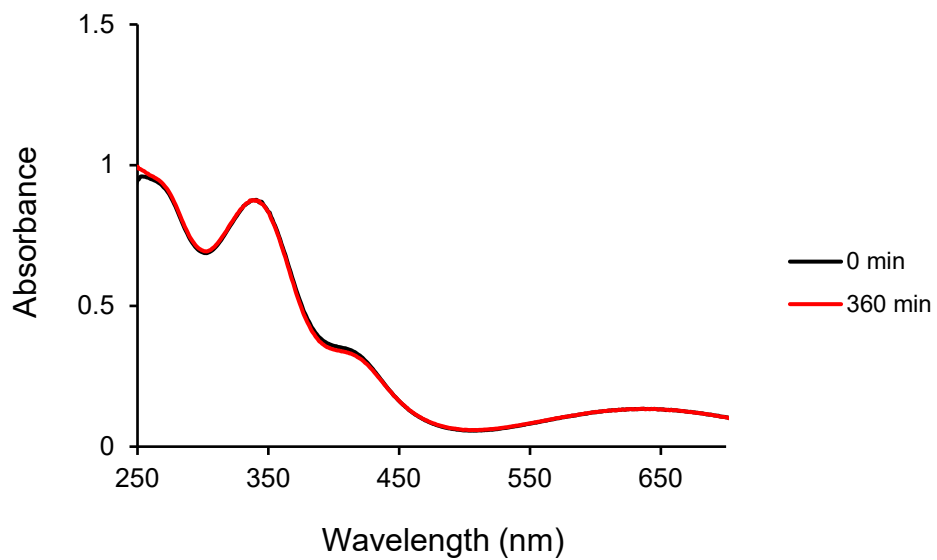


**Figure S12.** UV-Vis spectra of complex **C3** (100  $\mu$ M) incubated in PBS (pH 7.4) at 37 °C for 6 hours.

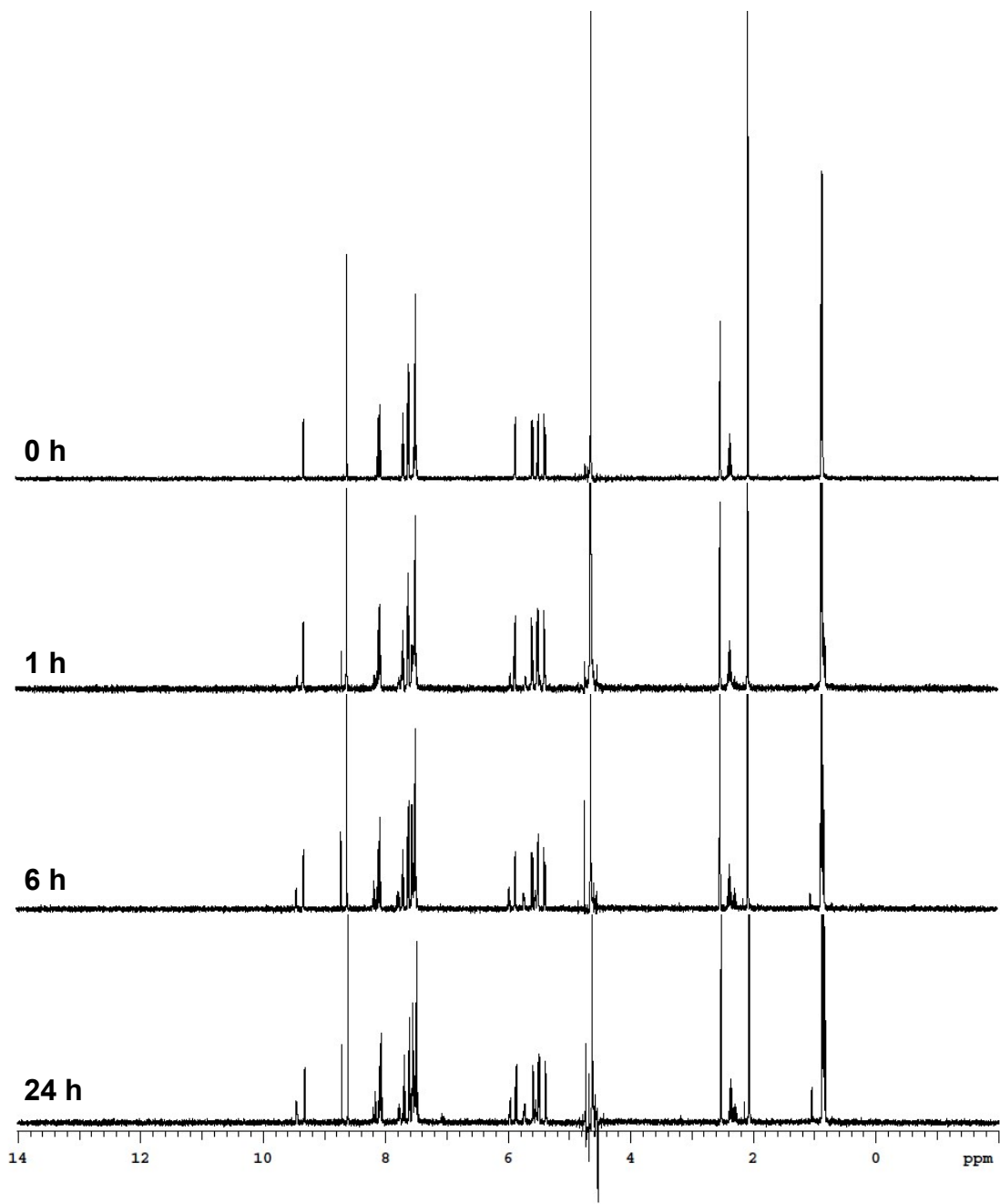


**Figure S13.** <sup>1</sup>H NMR of **C1** in D<sub>2</sub>O and 10% D<sub>6</sub>-DMSO over prolonged periods of incubation at 37°C.

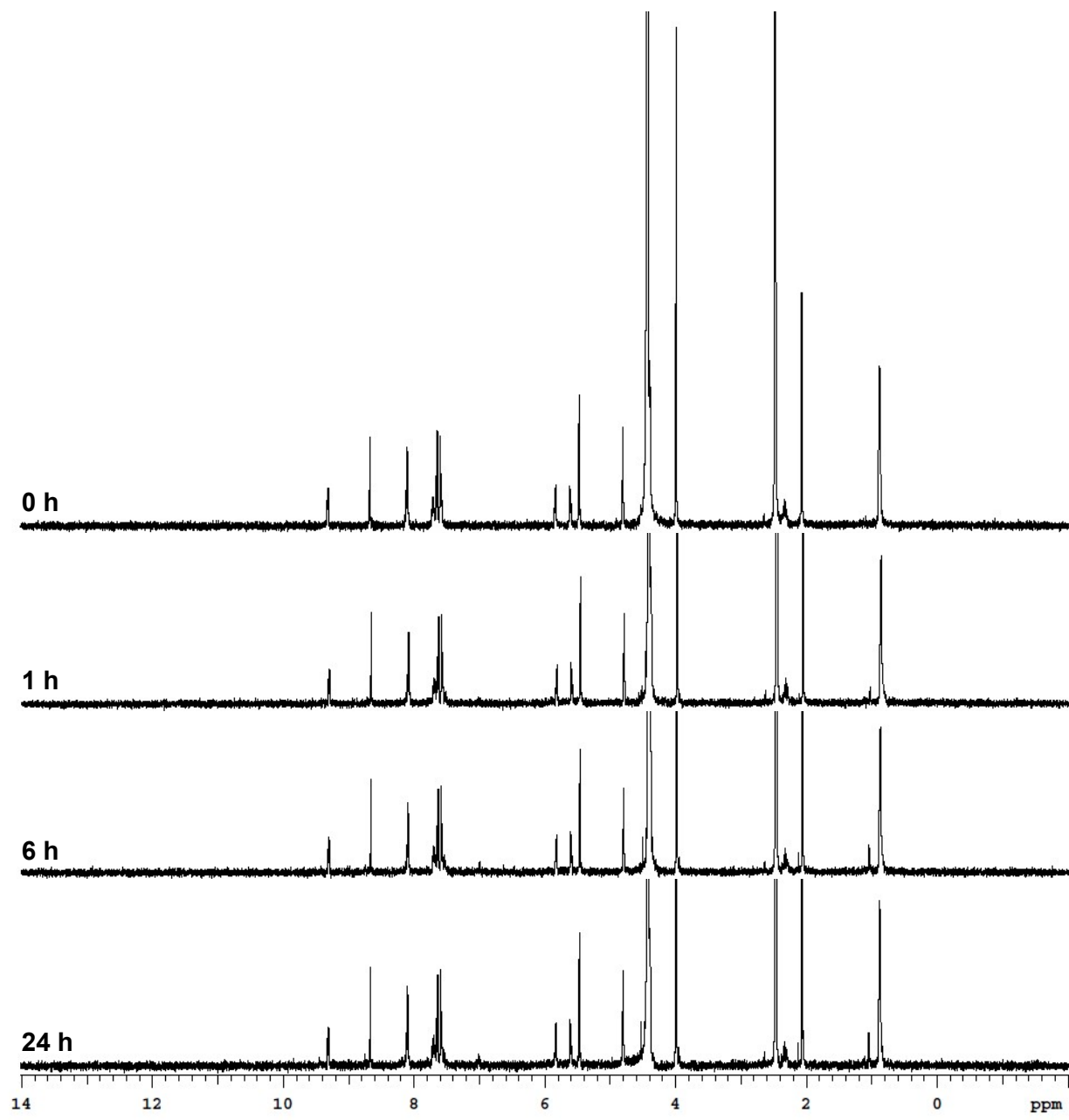


**Figure S14.** <sup>1</sup>H NMR of **C2** in D<sub>2</sub>O and 50% D<sub>6</sub>-DMSO over prolonged periods of incubation at 37°C.

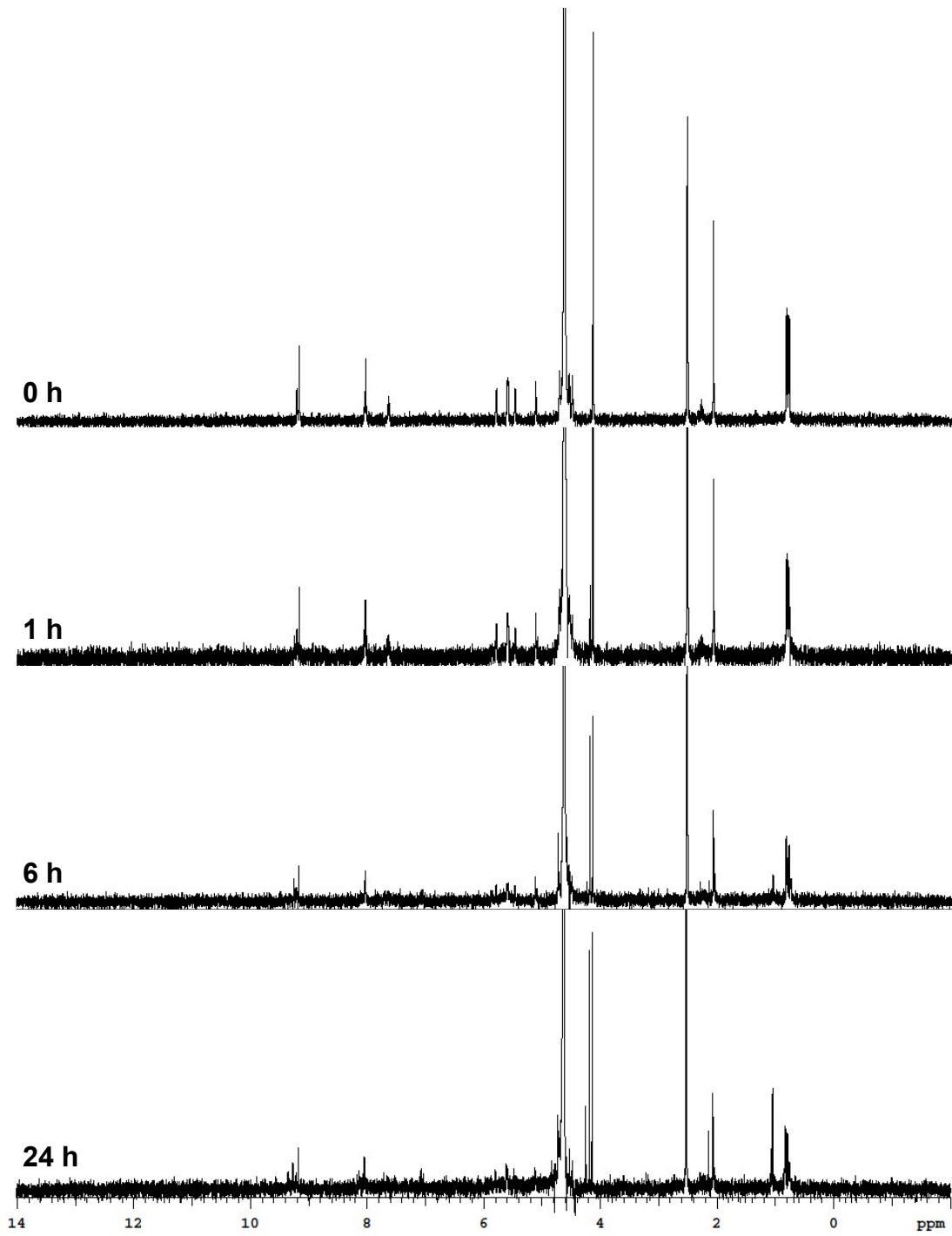


**Figure S15.** <sup>1</sup>H NMR of C3 in D<sub>2</sub>O and 10% D<sub>6</sub>-DMSO over prolonged periods of incubation at 37°C.

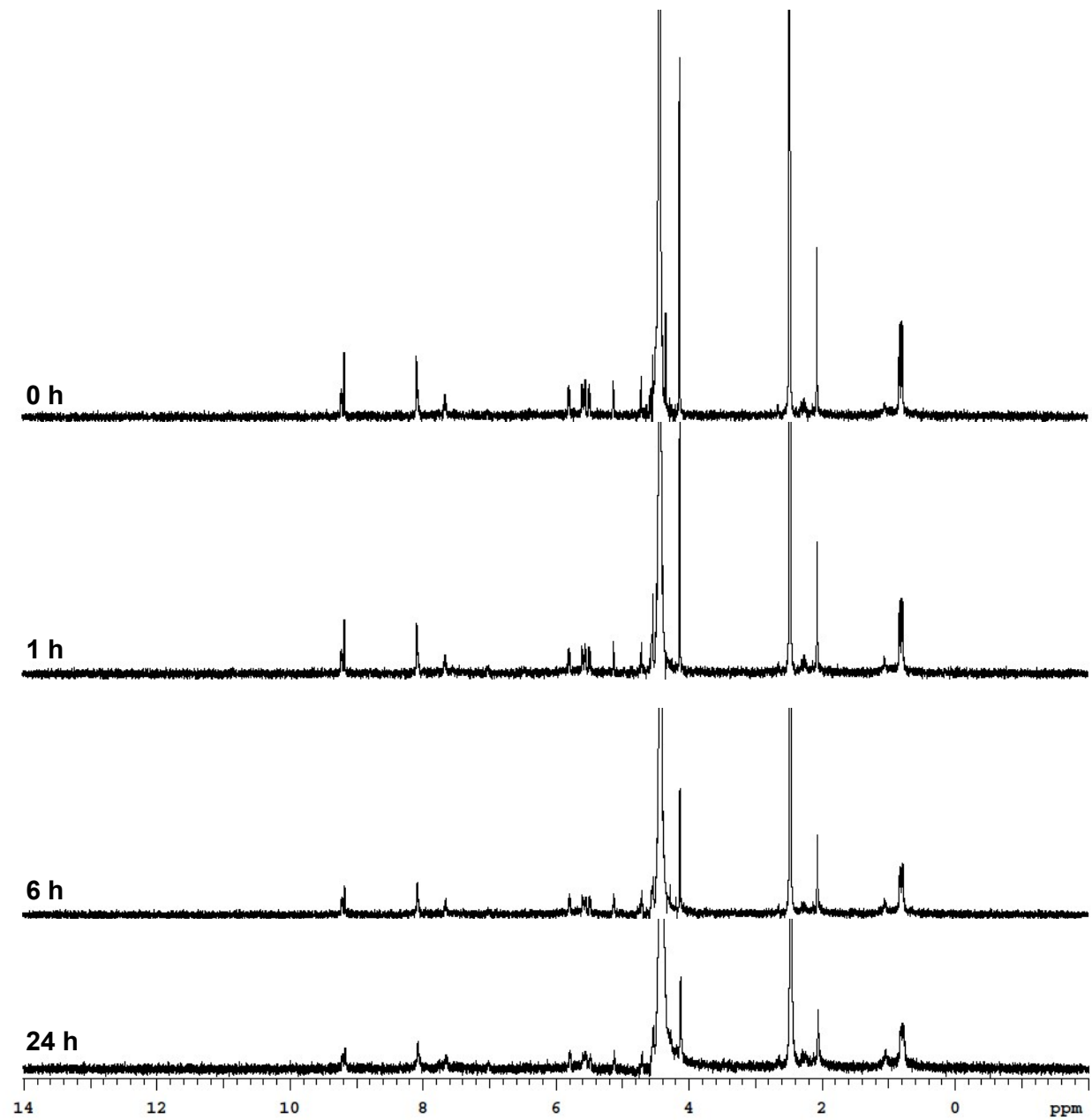


**Figure S16.** <sup>1</sup>H NMR of C3 in D<sub>2</sub>O and 50% D<sub>6</sub>-DMSO over prolonged periods of incubation at 37°C.

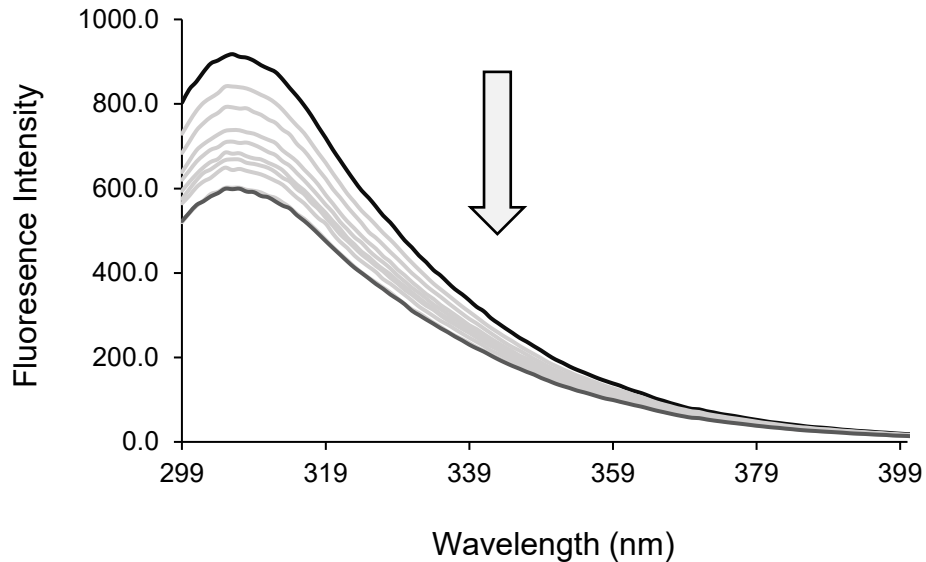


**Figure S17.** Fluorescence emission spectra at various complex-to-HSA ratios by the titration of HSA with **C1** using  $\lambda_{\text{ex}} = 260 \text{ nm}$  where the [HSA] = 10  $\mu\text{M}$  and the [Ru] = 0-25  $\mu\text{M}$ .

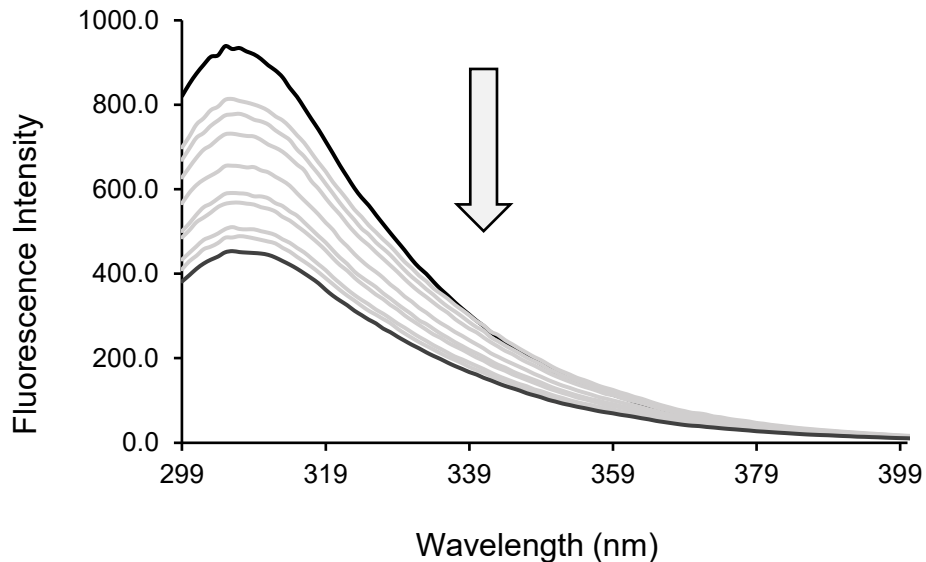


**Figure S18.** Fluorescence emission spectra at various complex-to-HSA ratios by the titration of HSA with **C2** using  $\lambda_{\text{ex}} = 260 \text{ nm}$  where the [HSA] = 10  $\mu\text{M}$  and the [Ru] = 0-25  $\mu\text{M}$ .

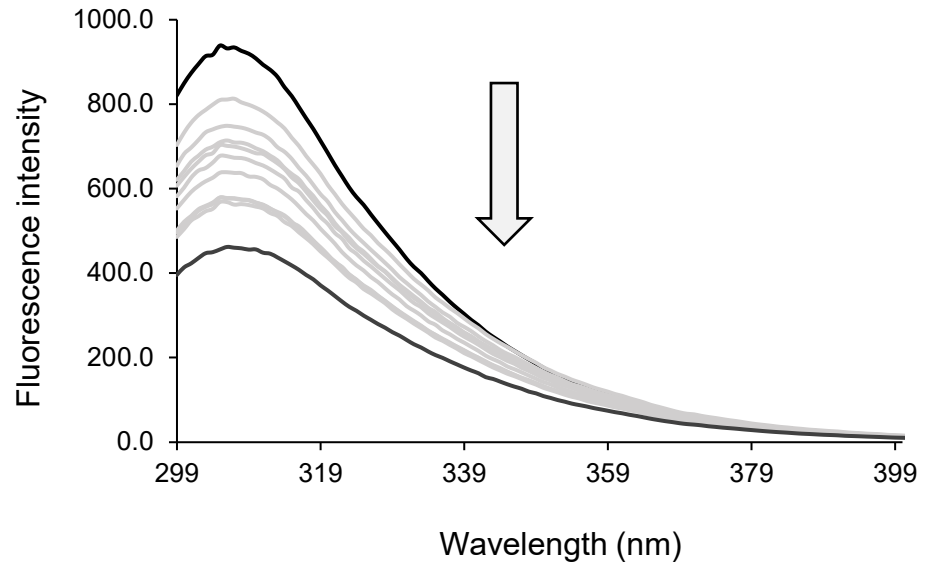


**Figure S19.** Fluorescence emission spectra at various complex-to-HSA ratios by the titration of HSA with **C3** using  $\lambda_{\text{ex}} = 260 \text{ nm}$  where the  $[\text{HSA}] = 10 \mu\text{M}$  and the  $[\text{Ru}] = 0\text{--}25 \mu\text{M}$ .

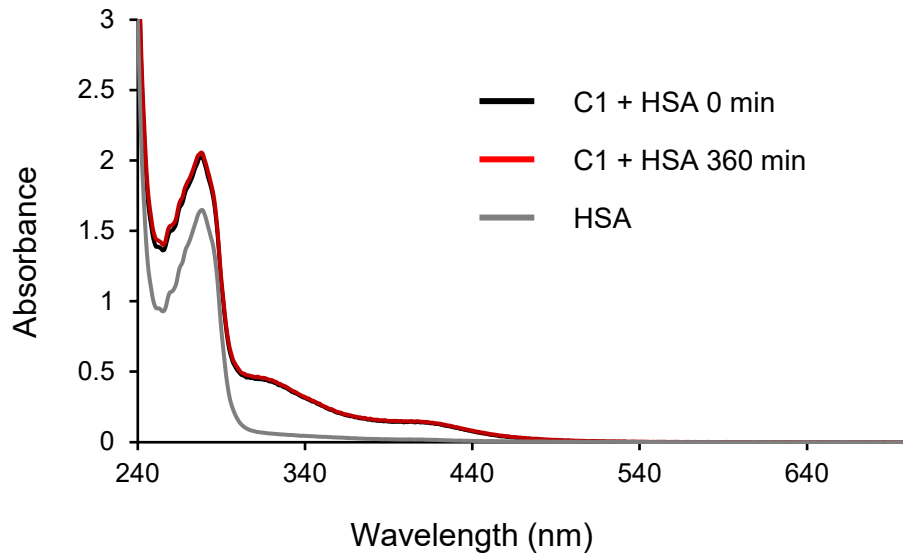


**Figure S20.** UV-Vis spectra of complex **C1** (50  $\mu\text{M}$ ) incubated with HSA (50  $\mu\text{M}$ ) in PBS buffer (pH 7.4) for 6 hours at 37  $^{\circ}\text{C}$ .

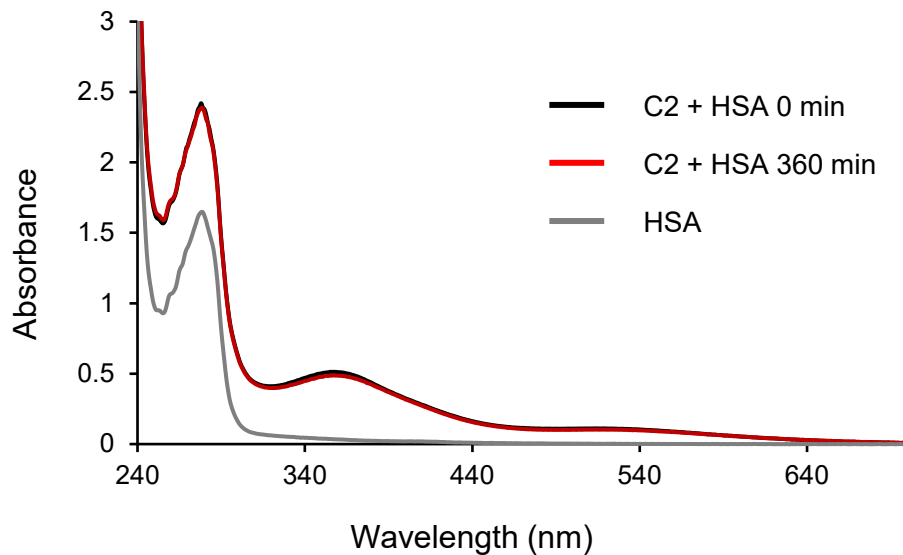


**Figure S21.** UV-Vis spectra of complex **C2** (50  $\mu\text{M}$ ) incubated with HSA (50  $\mu\text{M}$ ) in PBS buffer (pH 7.4) for 6 hours at 37  $^{\circ}\text{C}$ .

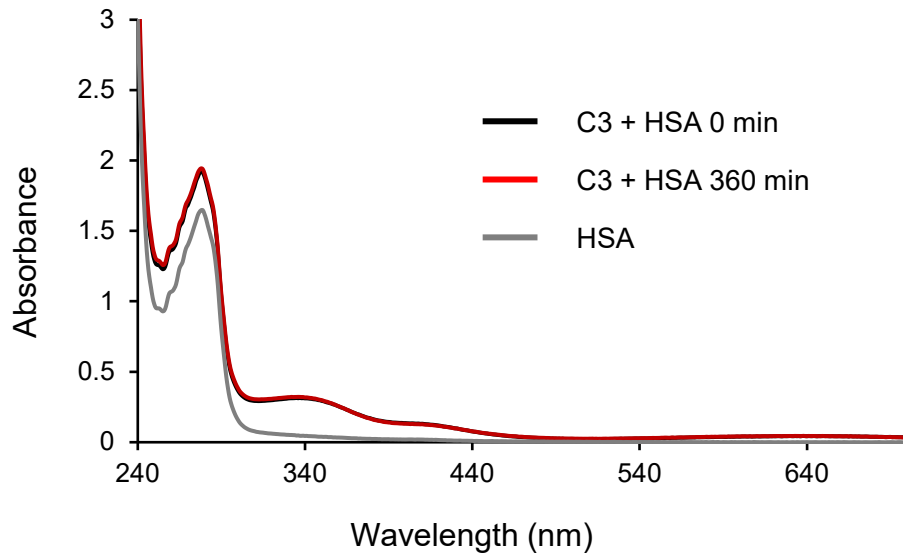


**Figure S22.** UV-Vis spectra of complex **C3** (50  $\mu\text{M}$ ) incubated with HSA (50  $\mu\text{M}$ ) in PBS buffer (pH 7.4) for 6 hours at 37  $^{\circ}\text{C}$ .

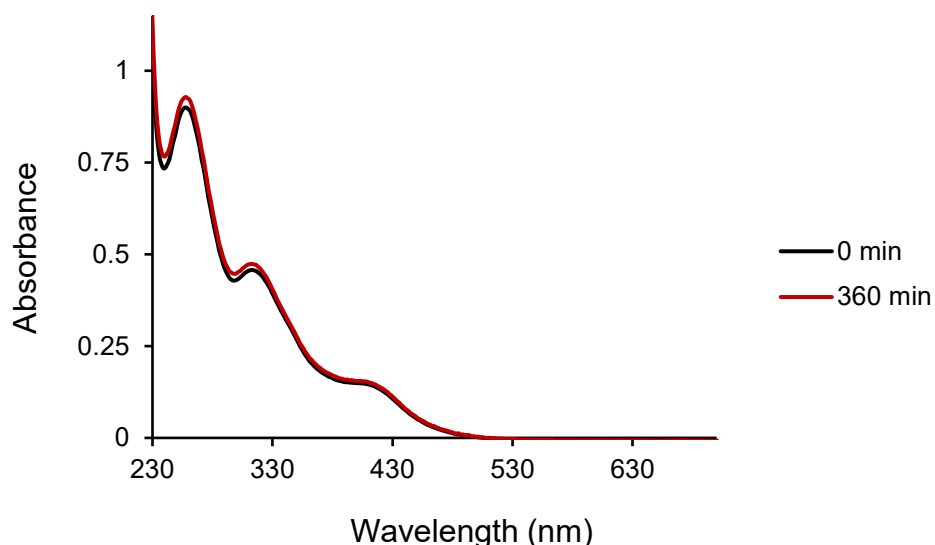


**Figure S23.** UV-Vis spectra of complex **C1** (50  $\mu$ M) incubated with CT-DNA (50  $\mu$ M) in Tris-HCl buffer (pH 7.0) for 6 hours at 37 °C.

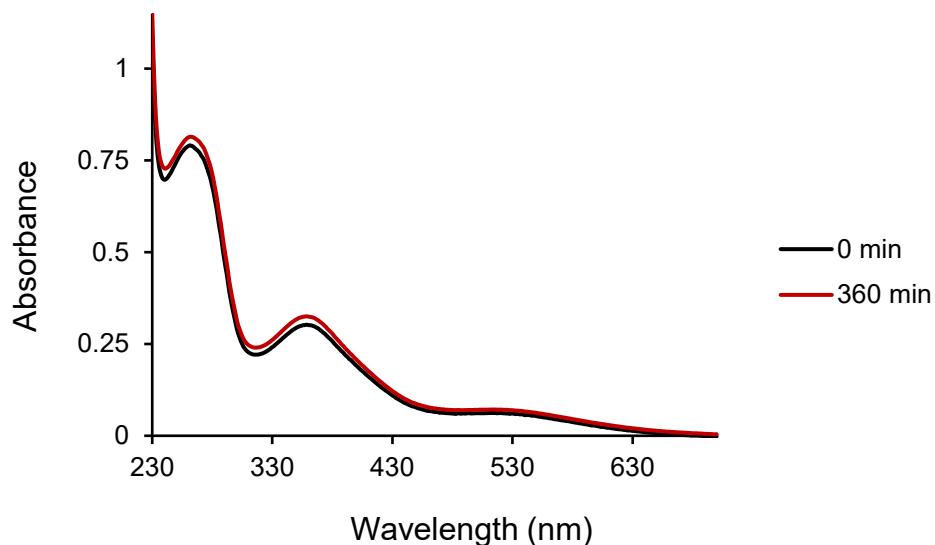


**Figure S24.** UV-Vis spectra of complex **C2** (50  $\mu$ M) incubated with CT-DNA (50  $\mu$ M) in Tris-HCl buffer (pH 7.0) for 6 hours at 37 °C.

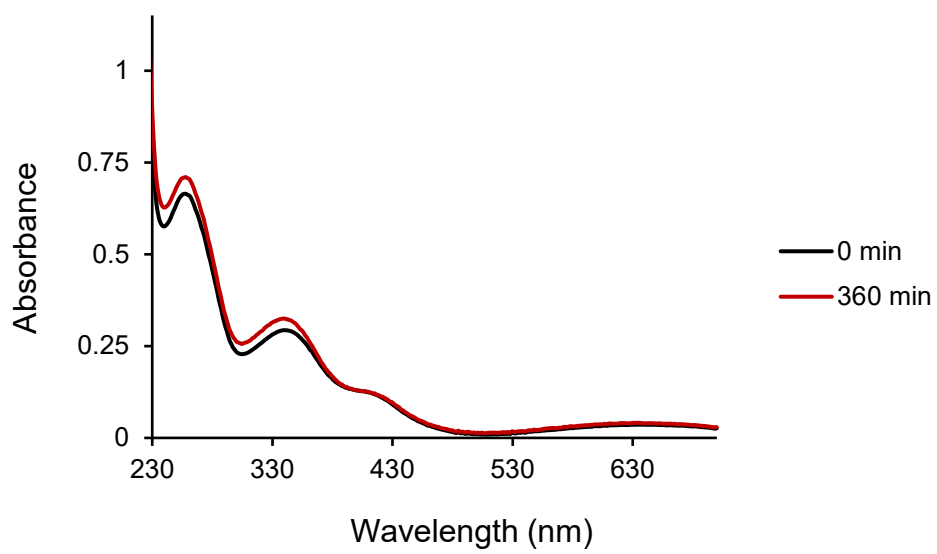


**Figure S25.** UV-Vis spectra of complex **C3** (50  $\mu$ M) incubated with CT-DNA (50  $\mu$ M) in Tris-HCl buffer (pH 7.0) for 6 hours at 37 °C.

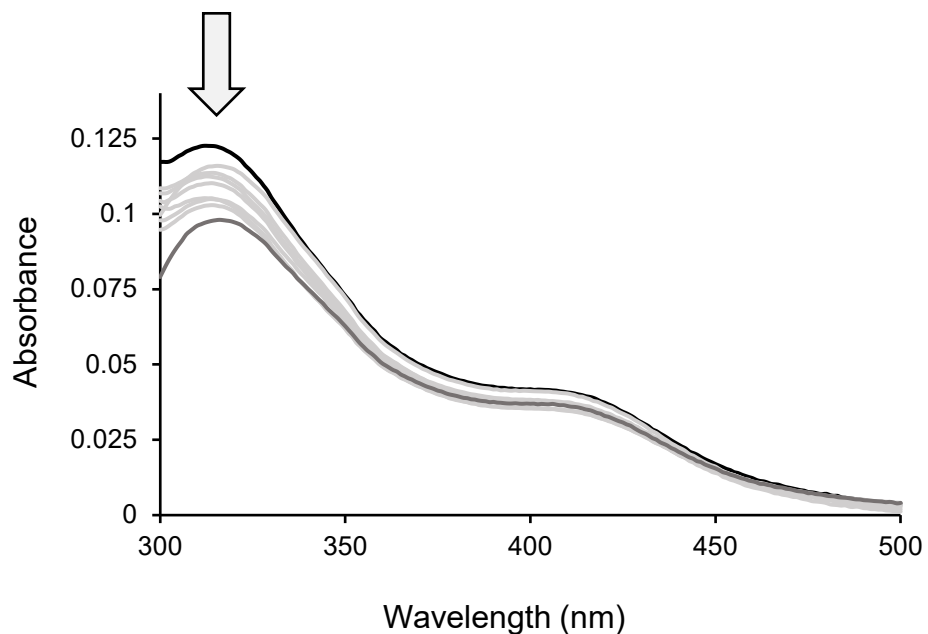


**Figure S26.** UV-Vis spectra of complex **C1** (30  $\mu\text{M}$ ) with CT-DNA (0 - 90  $\mu\text{M}$ ) in Tris-HCl buffer (pH 7.0) after 1 hour of incubation at 37 °C.

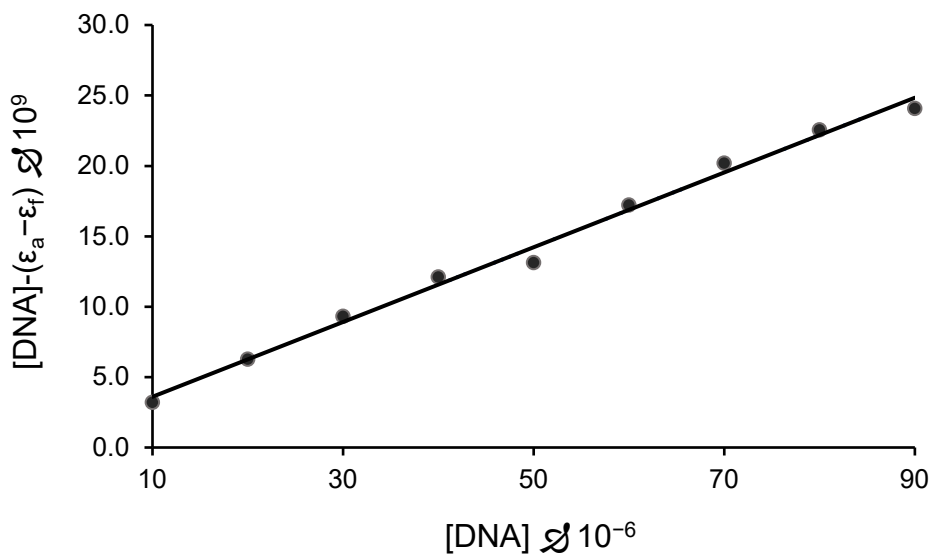


**Figure S27.** Plot of  $[DNA] / (\varepsilon_a - \varepsilon_f)$  versus  $[DNA]$  for the titration of **C1** with CT-DNA.

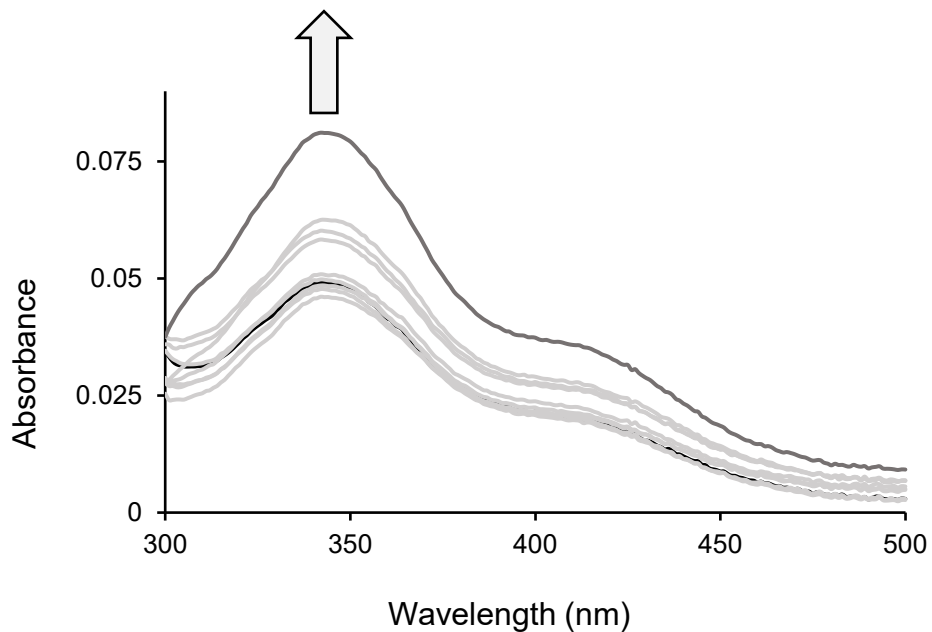


**Figure S28.** UV-Vis spectra of complex **C3** (30  $\mu\text{M}$ ) with CT-DNA (0 - 90  $\mu\text{M}$ ) in Tris-HCl buffer (pH 7.0) after 1 hour of incubation at 37  $^{\circ}\text{C}$ .

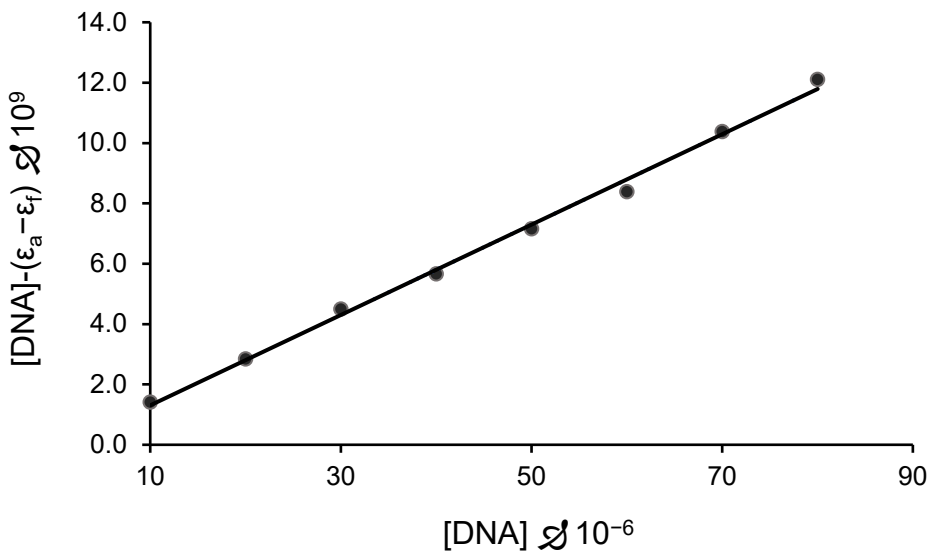


**Figure S29.** Plot of  $[\text{DNA}] / (\epsilon_A - \epsilon_f)$  versus  $[\text{DNA}]$  for the titration of **C3** with CT-DNA.

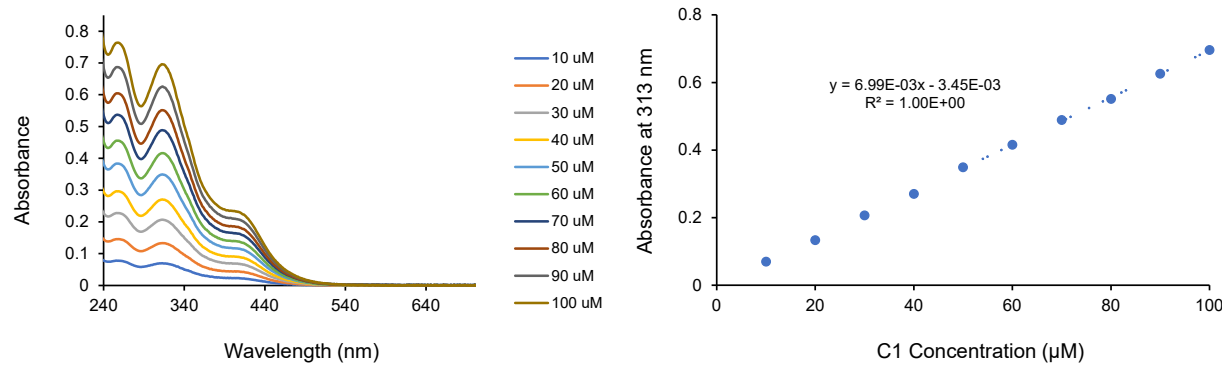


**Figure S30.** Calibration curve of **C1** in PBS (pH 7.4) to determine the extinction coefficient.

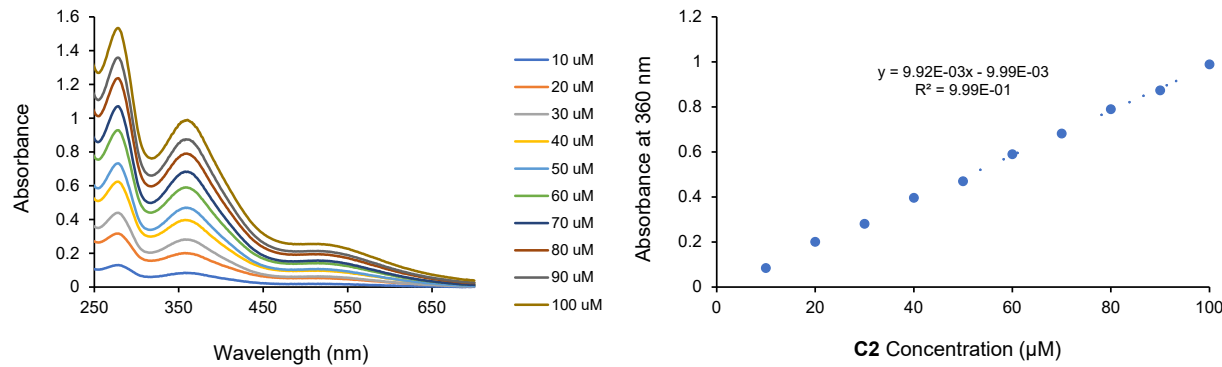


**Figure S31.** Calibration curve of **C2** in PBS (pH 7.4) to determine the extinction coefficient.

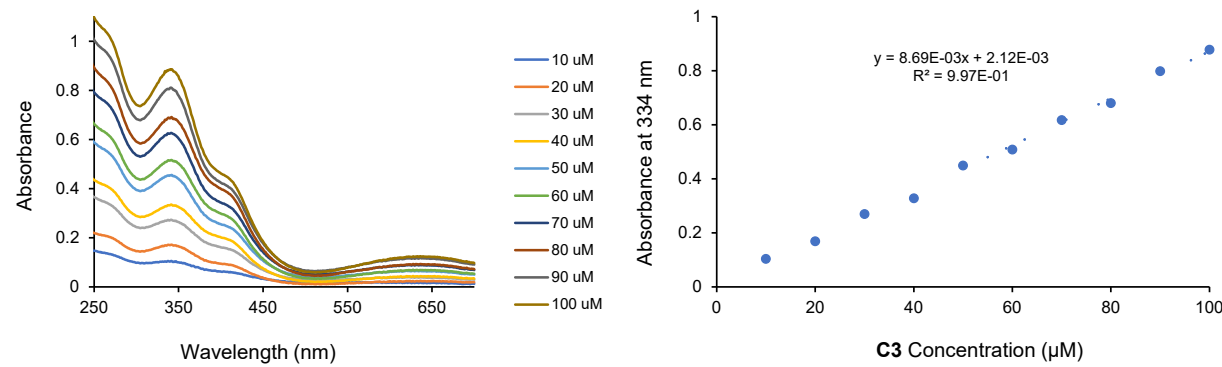


**Figure S32.** Calibration curve of **C3** in PBS (pH 7.4) to determine the extinction coefficient.

**Table S1.** Crystallographic data for complexes **C1** and **C3**.

	<b>C1</b>	<b>C3</b>
CCDC Number	2192092	2013493
molecular formula	$\text{C}_{22}\text{H}_{24}\text{ClF}_6\text{N}_2\text{PRu} \cdot \text{C}_3\text{H}_6\text{O}$	$\text{C}_{26}\text{H}_{28}\text{ClF}_6\text{FeN}_2\text{PRu}$
fw	656.00	705.84
crystal size (mm)	$0.36 \times 0.12 \times 0.05$	$0.37 \times 0.34 \times 0.32$
temp (K)	100(2)	100(2)
Crystal system	Triclinic	Monoclinic
space group	P1bar	$P2_1/c$
$a$ (Å)	9.1814(8)	18.600(2)
$b$ (Å)	12.3291(11)	20.872(2)
$c$ (Å)	12.6542(12)	13.7091(12)
$\alpha$ (°)	76.919(5)	90
$\beta$ (°)	73.108(5)	88.123(7)
$\gamma$ (°)	87.998(5)	90
$V$ (Å <sup>3</sup> )	1334.3(2)	5319.3(10)
Z	2	8
Wavelength (Å)	0.71073	0.71073
$\rho_{\text{calcd}}$ (g/cm <sup>3</sup> )	1.633	1.763
$\mu$ (mm <sup>-1</sup> )	0.812	1.336
$\theta$ range	1.70 – 27.73	1.10 – 32.12
refl. collected	43026	18735
indep. refl. / $R_{\text{int}}$	6226 / 0.030	18735 / 0.031
data/restraints/ parameters	43026 / 6226 / 0	18735 / 804 / 295
$R$ indices [ $ I  > 2\sigma(I)$ ]; $R_1/wR_2$	0.0199 / 0.0466	0.0306 / 0.0773
$R$ indices all data; $R_1/wR_2$	0.0234 / 0.0482	0.0417 / 0.0844
largest peak/hole (eÅ <sup>-3</sup> )	0.703 / -0.409	0.977 / -0.678
GOF	1.035	1.079